Molecular Sensing with Hyperpolarized 129Xe

Subjects: Chemistry, Applied

Contributor: Jabadurai Jayapaul , Leif Schröder

Hyperpolarized noble gases have been used early on in applications for sensitivity enhanced NMR. 129Xe has been explored for various applications because it can be used beyond the gas-driven examination of void spaces. Its solubility in aqueous solutions and its affinity for hydrophobic binding pockets allows "functionalization" through combination with host structures that bind one or multiple gas atoms. Moreover, the transient nature of gas binding in such hosts allows the combination with another signal enhancement technique, namely chemical exchange saturation transfer (CEST). Different systems have been investigated for implementing various types of so-called Xe biosensors where the gas binds to a targeted host to address molecular markers or to sense biophysical parameters.

Applied chemistry NMR molecular imaging

1. Introduction

Despite its excellent molecular specificity, NMR has strong limitations for many applications due to its low sensitivity at physiological conditions. The Boltzmann distribution around room temperature yields detectable magnetization for Faraday induction only if the spin densities are relatively high. This limitation is an even greater challenge for MRI and has been an active field of research for a long time. In this regard, the use of hyperpolarization techniques has opened up new possibilities in medical imaging diagnostics [1][2]. These techniques are key contributions to unleash the full analytical and diagnostic potential that is inherent to the NMR signal, particularly in biomedical applications. Conventional contrast agents act as relaxivity agents on the bulk water pool. They often require (a) relatively high concentrations (e.g., 10–100 µM for Gd-based T_1 agents) and (b) come with limited specificity. The strong background signal of ubiquitous tissue water is also of concern for certain applications. It can be addressed by detecting nuclei other than the abundant ^{1}H. Fluorine (^{19}F) NMR has been used in many studies [3] as a background-free option but still does not solve the sensitivity issue with regard to minimum detectable concentrations. The hyperpolarization of various nuclei, incl. ^{3}He, ^{13}C, ^{15}N, ^{129}Xe has thus attracted much attention over the recent years.

Hyperpolarized (hp) reporters based on ^{13}C and ^{15}N detection rely on covalently bound NMR-active atoms. They are used for real-time metabolic imaging to follow conversion of a metabolically active tracer (e.g., ^{13}C-labelled pyruvate) for visualizing the Warburg effect in oncology applications [1][4][5] or for visualizing metabolic turnover in the heart [6][7][8]. The noble gases He and Xe, however, have been used in rather different contexts as they are not part of any biologically relevant molecules. Hp ^{3}He has been applied early on for diagnostic lung imaging but is increasingly replaced with ^{129}Xe for such purposes [9]. Contrary to He, Xe has a decent solubility in aqueous

solutions and has thus also been used in structural biology studies to explore cavities in proteins [10]. Moreover, the investigation of porous materials also benefits from Xe NMR studies where the nucleus is sensitive to interactions with the wall material [11]. Thus, despite being an inert gas, ^{129}Xe is a valuable diagnostic and biomolecular reporter for exploring its molecular environment [12][13] as it combines high sensitivity with high specificity. Its affinity to certain molecular environments has fostered further applications of hp Xe in which tailored host structures are utilized for detection through supramolecular inclusion complexes. Hp ^{129}Xe NMR also displays a broad chemical shift range of about 300 ppm related to xenon's large polarizable electron cloud. This large chemical shift range of Xe enables sensing of different chemical environments under biological solutions with high sensitivity. Many different bound Xe resonances are clearly separable within this chemical shift range and thus promote simultaneous detection of various Xe environments. This motivated the so-called "multiplexing" approach in analogy to different dye-based optical imaging [14][15]. Nanocarriers with Xe affinity have been designed to enable sensitivity-enhanced NMR of otherwise undetectable spin density. Such targeted Xe hosts are summarized as functionalized Xe biosensors that were first pursued by the Pines and Wemmer labs [16]. They have evolved over the past 20 years in different designs with constant improvement in sensitivity. A major step was the combination with indirect detection through saturation transfer [17], a concept that had also consequences for optimized host design.

Xe biosensors have now been implemented for many different biological targets and their molecular properties have been studied under various conditions. As the concept moves towards preclinical applications, certain criteria have been identified to unleash the full potential that this method has shown in in vitro experiments for translation into biomedical diagnostics.

2. Xenon-Host Interactions: The Basis for Functionalized ^{129}Xe NMR

As a gas, Xe is a straightforward reporter for investigating cavities in porous materials [11]. Its application range, however, goes far beyond synthetic structures. Various proteins also have an affinity for Xe. Their complexes with the noble gas have been investigated in X-ray crystallography where Xe serves as a heavy element surrogate probe for O_2 binding sites in gas binding proteins [18][19][20]. The non-polar, inert guest can be a very powerful probe to explore host cavities that are otherwise occupied by guests but that do not yield a useful reporter signal. Together with its large chemical shift range as a consequence of its large polarizable electron cloud [21], Xe is a highly sensitive NMR reporter for cases where transient binding occurs. Identifying suitable host structures is a key step in designing Xe biosensors and various designs have been proposed. Importantly, both the binding affinity and the exchange kinetics are relevant for efficient molecular sensing.

3. Production and In Situ Delivery of hp Xe

The Zeeman splitting of nuclear spin states is a minor energy correction term in technically achievable external fields. While this is an advantage with respect to the harmless RF irradiation that is used to acquire NMR/MRI data,

it has major consequences for the achievable spin polarization at room temperature. Under thermal equilibrium conditions at ~300 K, the high temperature approximation applies and the system provides a rather minute "thermal polarization" in the presence of an external magnetic field. Thus, the NMR signal of dilute molecules is only detectable after extensive signal averaging and rather low SNR values. A higher concentration of the molecule of interest is typically unavoidable in order to achieve the desired NMR signal under thermal polarization conditions. To boost NMR sensitivity and to rapidly acquire signals with high SNR, hyperpolarization (hp) is actively being utilized for different reporter molecules. In hp conditions, the nuclear magnetization is artificially enhanced prior to the NMR experiment. Generally, the process provides 10^3–10^5 fold higher signal enhancement compared to the thermal polarization [5][13][22][23]. Electromagnetic radiation on the nuclear Larmor frequency cannot be used to directly overpopulate a spin state. Instead, all hyperpolarization techniques have in common that they rely on a precursor system that is polarized in a first step before the polarization is transferred onto the detected nuclei [5]. Two of the common hp approaches, DNP (dynamic nuclear polarization) and PHIP/SABRE (para-hydrogen induced polarization/signal amplification by reversible exchange), polarize covalently bound nuclei and thus the delivered tracer is part of the entire polarization procedure. Conversely, hyperpolarized ^{129}Xe gas can be generated without being covalently bound to the (indirectly) detected molecular structure.

Xe biosensors particularly rely on the concept that, only the noble gas undergoes the hp procedure and it is also delivered separately from the molecular host structure. This means that the preparation of the detected spin species happens entirely in the gas phase, followed by dispersion of Xe into the solution or sample of interest. The first step occurs via spin exchange optical pumping (SEOP) to transfer spin polarization from alkali metal vapor electrons (typically Rb) to Xe nuclear spins that are in transient contact with the alkali metal. Modern powerful laser systems (emission at 795 nm for the Rb D_1 transition) enable spin polarization between 20% and almost 100%.

4. Signal Transfer Detection Concepts for Xe

Although the preparation of Xe as a hp spin system provides a significant signal enhancement, the nuclei are not necessarily detected directly in a conventional NMR spectrum. Especially for studies with Xe dissolved in solutions containing other molecules of interest, the interactions of Xe with other nuclei might provide routes of signal transfer detection that also come with enhancement. This can include polarization transfer from protons with a larger Zeeman splitting or, vice versa, from hp Xe onto nearby nuclei. Another option is the signal transfer between multiple Xe pools that differ by chemical shift and exist as an abundant pool for detection that is in chemical exchange with dilute pools representing interaction partners of Xe. The latter method is called chemical exchange saturation transfer (CEST), which is also a widely used method in ^{1}H NMR and MRI.

5. Aspects of ^{129}Xe Biosensor Design

The key elements of Xe biosensors comprise the Xe host, a tether or spacer, and the ligand for a certain molecular target [16]. The development focusing on certain building blocks fostered strategies in which these units are typically combined on a scaffold or backbone and often include a fluorophore for cytometry to check for binding specificity

(see Figure 1a). Peptide synthesis concepts are often used for the coupling but modular approaches as illustrated in Figure 1b are also an option. Many of the early known Xe interaction partners show an unspecific binding and/or rapid exchange with no dedicated NMR resonance of bound Xe that can be used for CEST detection. The observation of reversible formation of a Xe@cryptophane inclusion complex in solution [24] fostered the idea to further develop this concept into a sensing platform. Cryptophanes with their tailored cavity sizes have thus been used in many sensor designs as starting material for coupling with binding motifs for different biological targets [15][25][26][27][28][29]. Further development of the HyperCEST approach, however, showed that there are other hosts with better Xe exchange dynamics [30][31][32][33].

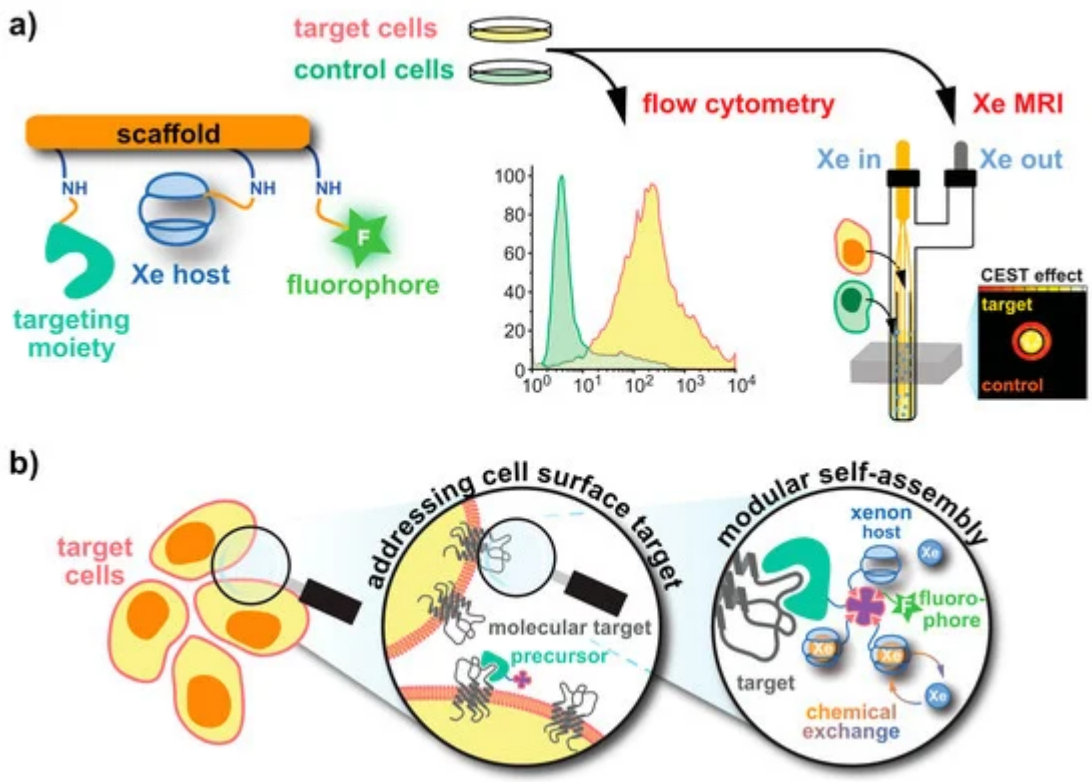

Figure 1. Strategies for obtaining functionalized Xe sensors. (**a**) A Xe host and targeting unit can be coupled to a (peptidic) scaffold via peptide synthesis at activatable tethers (orange). An optional dye label enables combined fluorescence and MRI specificity tests. (**b**) In a modular approach, a functionalized precursor (e.g., an avidin-activated binding motif) can be delivered to the target. Subsequent delivery of biotinylized Xe hosts and dyes yields the complete sensor.

6. Quantitative Analysis of ^{129}Xe Host Systems

In many studies, NMR and MRI are used as analytical tools where differences in signal intensities are observed but not necessarily analyzed to obtain absolute numbers for certain physical or chemical quantities. While this qualitative interpretation has been sufficient for many applications, there is an increasing interest in evaluating certain characteristic parameters on the molecular level to compare signal differences in different samples and between different setups.

In this context, computational efforts have been made for quantitative analysis of CEST responses. The saturation transfer comes with the advantage that the signal contrast can be controlled through the saturation duration (t_{sat}) and power (B_1). It is thus possible to characterize the exchanging host-guest system by applying different saturation conditions and analyzing the spectral response. The time-dependent magnetization components for two exchange-connected pools *A* and *B* that are exposed to a saturation pulse are described by the Bloch-McConnell equations [34]. Key parameters are the pool size of bound nuclei, f_B, the exchange rate k_{BA}, and the intrinsic relaxation times $T_{1/2}$ in both pools. The binding constant K_B can be derived from f_B for a given host concentration or, knowing the exchange kinetics and binding properties, the concentration of a host can be determined.

7. Translation Potential

NMR with hp ^{129}Xe has been long established for in vitro studies in the material sciences and through demonstrations of novel Xe biosensors. Regarding future applications of functionalized hp Xe in such sensors, biomedical studies in a preclinical context are the clear focus. This has also been the case for DNP and PHIP/SABRE applications, particularly for studies with ^{13}C-labelled pyruvate since the advent of dissolution DNP [35] and its continuous transition into clinical studies [36]. The DNP technique has been widely used to polarize ^{13}C or ^{15}N found in metabolites such that the change in metabolic activity linked to different diseases such as cancer or multiple sclerosis can be easily identified. A rather fast translation of DNP-mediated ^{13}C-metabolic findings into clinics was facilitated through continuous development of improved polarization of ^{13}C-labelled pyruvate, MRI optimizations, disease models, and biological insights achieved via various preclinical investigations. In spite of having several practical limitations, the recent advancement on DNP led to successful clinical trials, e.g., [1-^{13}C]-pyruvate trial in prostate cancer patients [37][36] and its further translation into clinical routine [38][39].

A critical point for the translation of the HyperCEST technique to (pre-)clinical applications is that this technique requires a certain time frame for building up the actively driven signal loss. A key component for future in vivo studies is thus the incorporation of host structures that provide a rather efficient exchange for optimum CEST effect. Additionally, clinical experience with MRI of dissolved Xe beyond lung tissue is still an emerging field of research that leaves room for improvement. Although improvements in SEOP setups and ^{129}Xe bio-carriers might facilitate the further translation, a successful demonstration of the Xe biosensor imaging at the desirable low concentrations in a pre-clinical setting is still lacking.

In preclinical studies, hp ^{129}Xe MRI has been utilized to validate different lung disease models, e.g., radiation induced lung injury (RILI), fibrotic lung tissue, elastic models of emphysema, asthma models, brain perfusion etc., noninvasively compared to tissue histology. By utilizing the sensitivity provided by hp ^{129}Xe MRI, the progress or changes in the disease patterns are monitored longitudinally in a more controlled way. Clinical lung imaging with Xe is already quite established and provides great anatomical and functional information [40][41]. It also served as a stepping stone for advanced clinical applications for mapping the Xe distribution in other organs like the human brain [42][43][44] as well as Xe MRI of the kidneys [45]. Additionally, hp ^{129}Xe MRI in the clinical side faces challenges similar to that of hp ^{13}C MRI, e.g., requiring optimization of dedicated RF coils for signal transmission/reception. Further, to sustain a longer T_1 time and polarization levels, the interaction of hp ^{129}Xe with oxygen during delivery

should be minimal. A vast majority of clinical research is performed on asthma and COPD disease models using hp ^{129}Xe MRI [2] where Xe has no extended contact time with oxygen within the blood or organs and MRI with Xe dissolved in such tissue is still being explored. A critical contribution is the parallel improvement of the technical components such as modern polarizers including high-performance laser diodes [46], optimized RF antenna systems [47][48], and adapted readout protocols. Any Xe MRI application benefits from such advancements, irrespective of being void space imaging or dissolved gas detection that ultimately also enables (pre)clinical biosensor studies. Recently, hp ^{129}Xe was utilized for the first time to quantify the gas exchange defects in a rat model of pulmonary hypertension [49]. Similarly, another (pre)clinical study reported the in vivo observation of ^{129}Xe HyperCEST responses after administering Sprague-Dawley (SD) rates with unfunctionalized CB[6] at millimolar concentrations [50]. Although this preliminary study provided insights on possible Xe distribution in highly perfused areas and nonspecific CB[6] accumulation in different organs, still there is a need for further improvements, e.g., MR sequence optimization, Xe carrier functionalization etc. to facilitate faster clinical translation. Such preclinical approaches might lead to testing different ^{129}Xe biosensors in vivo subsequently and to moving forward to the demonstration of molecular imaging applications of such probes. The full potential of hp ^{129}Xe NMR/MRI is not yet realized in the clinical stage due to an ongoing accumulation of sufficient and profound translation knowledge related to several components, including organ perfusion with Xe, polarizer optimization for CEST applications, biosafety of biosensors, pharmacokinetics etc. Compared to the other hp NMR techniques, the big advantage of Xe biosensors is the separate delivery of functionalized host units and hp nuclei. Figure 2 illustrates how this decoupling of the time scales for sensor delivery and hp lifetime immensely broadens the applications of hp MRI beyond metabolic imaging and will remain a driving force for further Xe biosensor development. The convenient timing for defining a diagnostic window together with simulations for highly efficient HyperCEST agents [51] pinpoint the way for diagnostic applications of functionalized Xe.

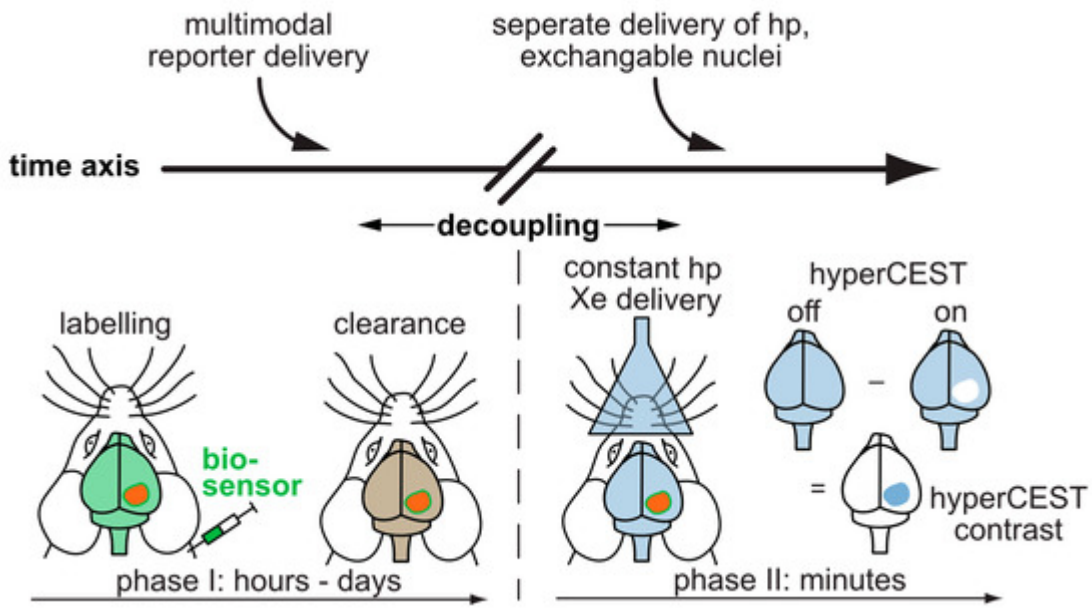

Figure 2. Translation of functionalized Xe to in vivo studies. The sensor is applied systemically and can accumulate in target tissue while wash-out occurs in the surrounding tissue. The decoupling of the time scales

allows to perform the more time-sensitive detection of hp ^{129}Xe in a second step. The hp ^{129}Xe can be delivered via inhalation and visualized in other highly perfused organs such as the brain.

8. Conclusions

The applications of hp ^{129}Xe nowadays go far beyond gas phase NMR/MRI. Since the pioneering work undertaken at UC Berkeley almost 20 years ago, the Xe biosensor concept has been constantly expanding. Advancements from Xe MRI in general (driven by lung imaging applications) and the overall success of the CEST approach in MRI have made important contributions to further pursue this diagnostic approach. The community is small but making important progress, as illustrated during regular meetings like the XeMat conference [52]. Neighboring disciplines like chemical engineering are invited to further promote this concept. At the same time, the sensing options with reversibly bound, hp ^{129}Xe could make novel contributions to characterize emerging materials like MOPs/MOFs or discover weak interactions in supramolecular systems. Taken together, the perspectives for detecting "functionalized Xe" with the HyperCEST method are promising for interdisciplinary work. Its high sensitivity can address previously inaccessible molecular systems, and this will continue to make NMR and MRI important analytical tools throughout the natural sciences and biomedical research communities.

References

1. Kurhanewicz, J.; Vigneron, D.B.; Ardenkjaer-Larsen, J.H.; Bankson, J.A.; Brindle, K.; Cunningham, C.H.; Gallagher, F.A.; Keshari, K.R.; Kjaer, A.; Laustsen, C.; et al. Hyperpolarized C MRI: Path to Clinical Translation in Oncology. Neoplasia 2019, 21, 1–16.
2. Adamson, E.B.; Ludwig, K.D.; Mummy, D.G.; Fain, S.B. Magnetic resonance imaging with hyperpolarized agents: methods and applications. Phys. Med. Biol. 2017, 62, R81–R123.
3. Ruiz-Cabello, J.; Barnett, B.P.; Bottomley, P.A.; Bulte, J.W.M. Fluorine 19F MRS and MRI in biomedicine. NMR Biomed. 2011, 24, 114–129.
4. Kurhanewicz, J.; Vigneron, D.B.; Brindle, K.; Chekmenev, E.Y.; Comment, A.; Cunningham, C.H.; DeBerardinis, R.J.; Green, G.G.; Leach, M.O.; Rajan, S.S.; et al. Analysis of Cancer Metabolism by Imaging Hyperpolarized Nuclei: Prospects for Translation to Clinical Research. Neoplasia 2011, 13, 81–97.
5. Witte, C.; Schröder, L. NMR of hyperpolarised probes. NMR Biomed. 2013, 26, 788–802.
6. Ball, D.R.; Cruickshank, R.; Carr, C.A.; Stuckey, D.J.; Lee, P.; Clarke, K.; Tyler, D.J. Metabolic imaging of acute and chronic infarction in the perfused rat heart using hyperpolarised [1-13C]pyruvate. NMR Biomed. 2013, 26, 1441–1450, doi:10.1002/nbm.2972.
7. Atherton, H.J.; Schroeder, M.A.; Dodd, M.S.; Heather, L.C.; Carter, E.E.; Cochlin, L.E.; Nagel, S.; Sibson, N.R.; Radda, G.K.; Clarke, K.; et al. Validation of the in vivo assessment of pyruvate

dehydrogenase activity using hyperpolarised 13C MRS. NMR Biomed. 2011, 24, 201–208.

8. Rider, O.J.; Tyler, D.J. Clinical Implications of Cardiac Hyperpolarized Magnetic Resonance Imaging. J. Cardiovasc. Magn. Reson. 2013, 15, 556.
9. Walkup, L.L.; Woods, J.C. Translational applications of hyperpolarized 3He and 129Xe. NMR Biomed. 2014, 27, 1429–1438.
10. Tilton, R.F., Jr; Kuntz, I.D., Jr Nuclear magnetic resonance studies of xenon-129 with myoglobin and hemoglobin. Biochemistry 1982, 21, 6850–6857.
11. Hollenbach, J.; Anger, B.; Matysik, J. Chapter 9. Probing Exchange and Diffusion in Confined Systems by 129Xe NMR Spectroscopy. In New Developments in NMR; Royal Society of Chemistry: Cambridge, UK, 2016; pp. 294–317.
12. Goodson, B.M. Nuclear magnetic resonance of laser-polarized noble gases in molecules, materials, and organisms. J. Magn. Reson. 2002, 155, 157–216.
13. Schröder, L. Xenon for NMR biosensing-inert but alert. Phys. Med. 2013, 29, 3–16.
14. Klippel, S.; Freund, C.; Schröder, L. Multichannel MRI labeling of mammalian cells by switchable nanocarriers for hyperpolarized xenon. Nano Lett. 2014, 14, 5721–5726.
15. Rose, H.M.; Witte, C.; Rossella, F.; Klippel, S.; Freund, C.; Schröder, L. Development of an antibody-based, modular biosensor for 129Xe NMR molecular imaging of cells at nanomolar concentrations. Proc. Natl. Acad. Sci. U. S. A. 2014, 111, 11697–11702.
16. Spence, M.M.; Rubin, S.M.; Dimitrov, I.E.; Ruiz, E.J.; Wemmer, D.E.; Pines, A.; Yao, S.Q.; Tian, F.; Schultz, P.G. Functionalized xenon as a biosensor. Proc. Natl. Acad. Sci. U. S. A. 2001, 98, 10654–10657.
17. Schroder, L.; Lowery, T.J.; Hilty, C.; Wemmer, D.E.; Pines, A. Molecular Imaging Using a Targeted Magnetic Resonance Hyperpolarized Biosensor. Science 2006, 314, 446–449.
18. Colloc'h, N.; Sopkova-de Oliveira Santos, J.; Retailleau, P.; Vivarès, D.; Bonneté, F.; Langlois d'Estainto, B.; Gallois, B.; Brisson, A.; Risso, J.-J.; Lemaire, M.; et al. Protein crystallography under xenon and nitrous oxide pressure: comparison with in vivo pharmacology studies and implications for the mechanism of inhaled anesthetic action. Biophys. J. 2007, 92, 217–224.
19. Cohen, J.; Arkhipov, A.; Braun, R.; Schulten, K. Imaging the migration pathways for O2, CO, NO, and Xe inside myoglobin. Biophys. J. 2006, 91, 1844–1857.
20. Johnson, B.J.; Cohen, J.; Welford, R.W.; Pearson, A.R.; Schulten, K.; Klinman, J.P.; Wilmot, C.M. Exploring molecular oxygen pathways in Hansenula polymorpha copper-containing amine oxidase. J. Biol. Chem. 2007, 282, 17767–17776.

21. Miller, K.W.; Reo, N.V.; Schoot Uiterkamp, A.J.; Stengle, D.P.; Stengle, T.R.; Williamson, K.L. Xenon NMR: chemical shifts of a general anesthetic in common solvents, proteins, and membranes. Proc. Natl. Acad. Sci. U. S. A. 1981, 78, 4946–4949.
22. Berthault, P.; Huber, J.G.; Desvaux, H. Biosensing using laser-polarized xenon NMR/MRI. Prog. Nucl. Magn. Reson. Spectrosc. 2009, 55, 35–60, doi:10.1016/j.pnmrs.2008.11.003.
23. Barskiy, D.A.; Coffey, A.M.; Nikolaou, P.; Mikhaylov, D.M.; Goodson, B.M.; Branca, R.T.; Lu, G.J.; Shapiro, M.G.; Telkki, V.-V.A.; Zhivonitko, V.V.; et al. Frontispiece: NMR Hyperpolarization Techniques of Gases. Chem. - A Eur. J. 2017, 23, 725–751, doi:10.1002/chem.201780461.
24. Bartik, K.; Luhmer, M.; Dutasta, J.-P.; Collet, A.; Reisse, J. 129Xe and1H NMR Study of the Reversible Trapping of Xenon by Cryptophane-A in Organic Solution. J. Am. Chem. Soc. 1998, 120, 784–791, doi:10.1021/ja972377j.
25. Seward, G.K.; Bai, Y.; Khan, N.S.; Dmochowski, I.J. Cell-compatible, integrin-targeted cryptophane-Xe NMR biosensors. Chem. Sci. 2011, 2, 1103–1110.
26. Witte, C.; Martos, V.; Rose, H.M.; Reinke, S.; Klippel, S.; Schröder, L.; Hackenberger, C.P.R. Live-cell MRI with xenon hyper-CEST biosensors targeted to metabolically labeled cell-surface glycans. Angew. Chem. Int. Ed Engl. 2015, 54, 2806–2810.
27. Boutin, C.; Stopin, A.; Lenda, F.; Brotin, T.; Dutasta, J.-P.; Jamin, N.; Sanson, A.; Boulard, Y.; Leteurtre, F.; Huber, G.; et al. Cell uptake of a biosensor detected by hyperpolarized 129Xe NMR: the transferrin case. Bioorg. Med. Chem. 2011, 19, 4135–4143.
28. Milanole, G.; Gao, B.; Paoletti, A.; Pieters, G.; Dugave, C.; Deutsch, E.; Rivera, S.; Law, F.; Perfettini, J.-L.; Mari, E.; et al. Bimodal fluorescence/129Xe NMR probe for molecular imaging and biological inhibition of EGFR in Non-Small Cell Lung Cancer. Bioorg. Med. Chem. 2017, 25, 6653–6660.
29. Schnurr, M.; Sydow, K.; Rose, H.M.; Dathe, M.; Schröder, L. Brain endothelial cell targeting via a peptide-functionalized liposomal carrier for xenon hyper-CEST MRI. Adv. Healthc. Mater. 2015, 4, 40–45.
30. Kunth, M.; Witte, C.; Hennig, A.; Schröder, L. Identification, classification, and signal amplification capabilities of high-turnover gas binding hosts in ultra-sensitive NMR. Chem. Sci. 2015, 6, 6069–6075.
31. Schnurr, M.; Sloniec-Myszk, J.; Döpfert, J.; Schröder, L.; Hennig, A. Supramolecular Assays for Mapping Enzyme Activity by Displacement-Triggered Change in Hyperpolarized 129Xe Magnetization Transfer NMR Spectroscopy. Angew. Chem. Int. Ed Engl. 2015, 54, 13444–13447.
32. Farhadi, A.; Ho, G.; Kunth, M.; Ling, B.; Lakshmanan, A.; Lu, G.; Bourdeau, R.W.; Schröder, L.; Shapiro, M.G. Recombinantly Expressed Gas Vesicles as Nanoscale Contrast Agents for Ultrasound and Hyperpolarized MRI. AIChE J. 2018, 64, 2927–2933.

33. Kunth, M.; Lu, G.J.; Witte, C.; Shapiro, M.G.; Schröder, L. Protein Nanostructures Produce Self-Adjusting Hyperpolarized Magnetic Resonance Imaging Contrast through Physical Gas Partitioning. Acs Nano 2018, 12, 10939–10948, doi:10.1021/acsnano.8b04222.
34. Kunth, M.; Schröder, L. CEST MRI. In Quantification of Biophysical Parameters in Medical Imaging; Springer Science and Business Media LLC: Cham, Switzerland, 2017; pp. 213–253.
35. Ardenkjær-Larsen, J.H.; Fridlund, B.; Gram, A.; Hansson, G.; Lerche, M.H.; Servin, R.; Thaning, M.; Golman, K.; Hansson, L. Increase in signal-to-noise ratio of > 10,000 times in liquid-state NMR. Proc. Natl. Acad. Sci. USA 2003, 100, 10158–10163, doi:10.1073/pnas.1733835100.
36. Nelson, S.J.; Kurhanewicz, J.; Vigneron, D.B.; Larson, P.E.Z.; Harzstark, A.L.; Ferrone, M.; van Criekinge, M.; Chang, J.W.; Bok, R.; Park, I.; et al. Metabolic imaging of patients with prostate cancer using hyperpolarized [1-13C]pyruvate. Sci. Transl. Med. 2013, 5, 198ra108.
37. Keshari, K.R.; Wilson, D.M. ChemInform Abstract: Chemistry and Biochemistry of 13 C Hyperpolarized Magnetic Resonance Using Dynamic Nuclear Polarization. Chemin 2014, 45, 1627–1659, doi:10.1002/chin.201418300.
38. Wang, Z.J.; Ohliger, M.A.; Larson, P.E.Z.; Gordon, J.W.; Bok, R.A.; Slater, J.; Villanueva-Meyer, J.E.; Hess, C.P.; Kurhanewicz, J.; Vigneron, D.B. Hyperpolarized C MRI: State of the Art and Future Directions. Radiology 2019, 291, 273–284.
39. Le Page, L.M.; Guglielmetti, C.; Taglang, C.; Chaumeil, M.M. Imaging Brain Metabolism Using Hyperpolarized 13C Magnetic Resonance Spectroscopy. Trends Neurosci. 2020, 43, 343–354.
40. Doganay, O.; Chen, M.; Matin, T.; Rigolli, M.; Phillips, J.-A.; McIntyre, A.; Gleeson, F.V. Magnetic resonance imaging of the time course of hyperpolarized Xe gas exchange in the human lungs and heart. Eur. Radiol. 2019, 29, 2283–2292.
41. Ruppert, K.; Qing, K.; Patrie, J.T.; Altes, T.A.; Mugler, J.P., 3rd Using Hyperpolarized Xenon-129 MRI to Quantify Early-Stage Lung Disease in Smokers. Acad. Radiol. 2019, 26, 355–366.
42. Rao, M.R.; Norquay, G.; Stewart, N.J.; Hoggard, N.; Griffiths, P.D.; Wild, J.M. Assessment of brain perfusion using hyperpolarized Xe MRI in a subject with established stroke. J. Magn. Reson. Imaging 2019, doi:10.1002/jmri.26686.
43. Chahal, S.; Prete, B.R.J.; Wade, A.; Hane, F.T.; Albert, M.S. Brain Imaging Using Hyperpolarized Xe Magnetic Resonance Imaging. Methods Enzymol. 2018, 603, 305–320.
44. Rao, M.R.; Stewart, N.J.; Griffiths, P.D.; Norquay, G.; Wild, J.M. Imaging Human Brain Perfusion with Inhaled Hyperpolarized Xe MR Imaging. Radiology 2018, 286, 659–665.
45. Chacon-Caldera, J.; Maunder, A.; Rao, M.; Norquay, G.; Rodgers, O.I.; Clemence, M.; Puddu, C.; Schad, L.R.; Wild, J.M. Dissolved hyperpolarized xenon-129 MRI in human kidneys. Magn. Reson. Med. 2019, doi:10.1002/mrm.27923.

46. Nikolaou, P.; Coffey, A.M.; Walkup, L.L.; Gust, B.M.; Whiting, N.; Newton, H.; Muradyan, I.; Dabaghyan, M.; Ranta, K.; Moroz, G.D.; et al. XeNA: an automated “open-source” 129Xe hyperpolarizer for clinical use. Magn. Reson. Imaging 2014, 32, 541–550.
47. Rao, M.; Stewart, N.J.; Norquay, G.; Griffiths, P.D.; Wild, J.M. High resolution spectroscopy and chemical shift imaging of hyperpolarized 129Xe dissolved in the human brain in vivo at 1.5 tesla. Magn. Reson. Med. 2016, 75, 2227–2234.
48. Asfour, A. A three-coil RF probe-head at 2.35 T: Potential applications to the 23Na and to the hyperpolarized 129Xe MRI in small animals.; IEEE, 2010; pp. 5693–5699.
49. Virgincar, R.S.; Nouls, J.C.; Wang, Z.; Degan, S.; Qi, Y.; Xiong, X.; Rajagopal, S.; Driehuys, B. Quantitative Xe MRI detects early impairment of gas-exchange in a rat model of pulmonary hypertension. Sci. Rep. 2020, 10, 7385.
50. Hane, F.T.; Li, T.; Smylie, P.; Pellizzari, R.M.; Plata, J.A.; DeBoef, B.; Albert, M.S. In vivo detection of cucurbit[6]uril, a hyperpolarized xenon contrast agent for a xenon magnetic resonance imaging biosensor. Sci. Rep. 2017, 7, 41027.
51. Shapiro, M.G.; Ramirez, R.M.; Sperling, L.J.; Sun, G.; Sun, J.; Pines, A.; Schaffer, D.V.; Bajaj, V.S. Genetically encoded reporters for hyperpolarized xenon magnetic resonance imaging. Nat. Chem. 2014, 6, 629–634, doi:10.1038/nchem.1934.
52. XeMat 2018 Speaker Abstracts Available online: https://cpb-us-w2.wpmucdn.com/web.sas.upenn.edu/dist/a/374/files/2018/05/SPEAKERS-XEMAT-2018-274k1mu.pdf (accessed on Feb 9, 2020).